

# Thickness dependent enhancement of the polar magneto-optic Kerr effect in Co magnetoplasmonic nanostructures

Emil Melander,<sup>1,\*</sup> Sebastian George,<sup>1</sup> Blanca Caballero,<sup>2</sup> Antonio García-Martín,<sup>2</sup>  
Björgvin Hjörvarsson,<sup>1</sup> Vassilios Kapaklis,<sup>1</sup> and Evangelos Th. Papaioannou<sup>3,†</sup>

<sup>1</sup>*Department of Physics and Astronomy, Uppsala University, Box 516, SE-751 20 Uppsala Sweden*

<sup>2</sup>*IMM-Instituto de Microelectronica de Madrid (CNM-CSIC),*

*Isaac Newton 8, PTM, Tres Cantos, E-28760 Madrid, Spain*

<sup>3</sup>*Fachbereich Physik and Forschungszentrum OPTIMAS Technische Universität, Kaiserslautern, 67663 Kaiserslautern, Germany*

We reveal the influence of the thickness of the ferromagnetic layer on the surface plasmon polariton assisted enhancement of the polar magneto-optic Kerr effect. The optical and magneto-optical response is strongly altered by the thickness of the magnetic layer as shown in specular reflectivity and polar magneto-optical Kerr effect measurements. That the main spectral feature of the magneto-optical enhancement does not only depend on the in-plane structuring of the sample but also on the out-of-plane geometrical parameters, such as the thickness. For the specific thickness of 100 nm for the Co layer an sixfold enhancement of the polar magneto-optical effect is observed, as compared to a continuous Co film of the same thickness.

## I. INTRODUCTION

Magnetoplasmonics is an emergent research field that aims to strongly modify the magneto-optic response in the presence of surface plasmons and to control plasmonic resonances with magnetic fields[1, 2]. The enhancement of the magneto-optical effects especially of the polar and transversal Kerr effect (PMOKE-TMOKE) due to the presence of surface plasmons has been shown in many different nanostructures. Examples are hybrid nanostructures of noble metal/ferromagnetic metal (or dielectric) like Co/Au, YIG/Au [3], in Au/Co/Au trilayers [4] and multilayers[5], as well as in patterned pure magnetic films [6–12]. The enhancement has been reported for both types of plasmonic excitations for localized (LSPs)- and for propagating (SPPs) surface plasmons [13–15]. The mechanism for the increased magneto-optical values is the enhancement of the electric field provided by the excitation of either localized plasmons or propagating plasmons, as very recently shown by correlating near-and far-field optical and magneto-optical response [15].

Despite the numerous studies on materials combinations and geometrical considerations little attention has been given to the parameter of the thickness of the magnetic layer. In Au/Co/Au trilayers [16] an optimum Co thickness for the redistribution of the electromagnetic field in the magnetic layer has been observed at around 8 nm when plasmon excitation is occurring at the Au/air interface. However, there is no such study for the case of pure magnetic nanostructures. In this paper we use hexagonal arrays of holes perforated in Co films of different thicknesses. We use optical reflectivity and polar magneto-optical Kerr effects together with simulations in order to reveal the dependence of the magneto-optic en-

hancement on the magnetic layer thickness. Our study is focused on relatively thick Co films with the film thickness,  $t$ , being smaller than the wavelength of the incident light  $\lambda$ , and larger than the skin depth  $\delta$  of the metal, i.e.  $\delta \leq t < \lambda$ . We show that thickness constitutes another way to manipulate the enhancement of the PMOKE signal.

Three Co films were patterned by the use of self-organization of colloidal polystyrene beads on Si substrates as shadow masks [7]. The final layout of the samples, is presented in fig. 1. The hexagonal hole structure has a periodicity of  $a_0 = 470(15)$  nm and hole sizes of  $d = 260(10)$ nm. A very thin buffer layer of Ti was initially deposited for better adhesion of the Co on the Si and Co layers with different thickness were grown on the seeding layer. To prevent oxidation of the Co surface, a capping layer of 2 nm Au was deposited. The final structure of the samples is: Au (2 nm)/Co (X nm)/Ti (2nm)/Si(111), with X being either 20, 60, or 100 nm. Continuous thin films of the same composition were prepared at the same time to be used reference samples.

There are two crystal directions that are relevant for plasmon excitation, being the nearest neighbour [10] and the second nearest neighbour [11] directions. These can be aligned parallel to the scattering plane in our experimental setup and we performed our measurements aligning the scattering plane to the [10] direction, as shown in Fig. 1.

For the PMOKE measurements white light from a mercury lamp source is used to obtain a broadband light spectrum. The light then is monochromatized by using a grating monochromator and afterwards sent first through a high-pass filter, to suppress the effects from higher harmonics, and thereafter through a set of beam-shaping and focusing lenses, to maximise the light intensity reaching the sample. To minimise the noise, the light is modulated with either a chopper or a Faraday cell. Before being reflected, the light is focused onto the sample with an angle

\* Corresponding author: Emil.Melander@physics.uu.se

† Corresponding author: epapa@physik.uni-kl.de

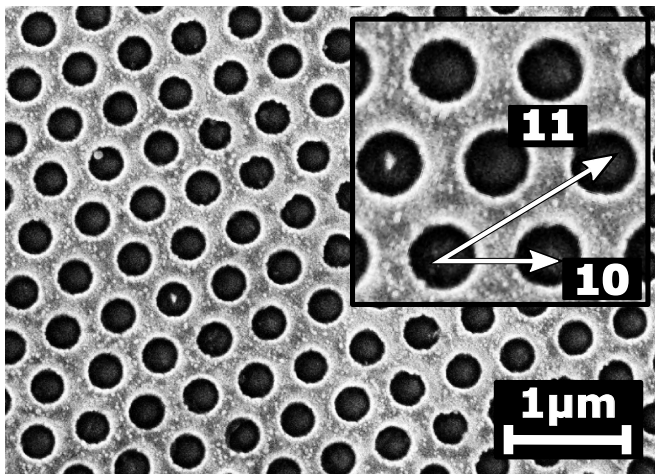


FIG. 1. A SEM image of a typical sample to show the overall uniformity of the structure. The inset shows the hexagonal hole arrangement in closer detail as well as the two main directions for plasmon excitations, which are available in this type of lattice[9].

of incidence of 4 degrees through a hole in the magnetic core of the ferromagnetic coils. The maximum magnetic field strength is 2.2 T. Finally the light goes through the automated polariser before being focused onto the detector. The modulated signal is measured using either a photo-detector or a photo-multiplier tube connected to a lock-in amplifier. For the spectral reflectivity the same setup is adjusted for reflectivity measurements by guiding the reflected light through a lens onto a photo-multiplier tube (PMT) or photo detector. The polar Kerr rotation is measured in absolute values (degrees), as it is measured after magnetically saturating the sample in the two polar directions and comparing the polarisation rotation difference, by scanning the polariser for the point of light extinction. In this work, reflectivity and polar Kerr-rotation measurements were performed in an energy range from 1 to 4.2 eV. Polar Kerr-rotation spectra were measured with the sample in a fully saturated magnetic state (applied magnetic field  $B = 1.1$  T).

Figure 2 (a) shows the calculated reflectivity, (c) the experimental reflectivity, (b) the calculated magneto-optical spectra for the three antidot samples, and (d) the MOKE spectra of the patterned samples in comparison with their corresponding continuous films. The reflectivity curves were obtained with p-polarized light and measured relative to the intensity of the direct beam. Figure 2 (c) shows that below 3 eV the main feature is the trough in reflectivity at  $\approx 2.81$  eV for the 60 nm sample and at  $\approx 2.69$  eV for the 100 nm. The trough is present but hardly visible for the sample with 20 nm Co thickness, however can be estimated to lie around 2.9 eV. The continuous reference films exhibit a typical metallic behaviour. A second broad and intense dip is appearing for energies  $\approx 3.75$  eV and  $\approx 4.0$  eV for the 100 nm and 60 nm respectively. Figure 2 (a) presents the calculated

reflectivity curves for the three samples. Apart from the 20 nm sample where the reflectivity of the Si substrate dominates, the calculation captures well the reflectivity behaviour of the samples. The observed minima in reflectivity for all the Co samples are the result of the resonant coupling of light to SPPs excitations at the Co / air patterned interfaces as it can numerically calculated by using the scattering matrix approach[17] and shown in Fig. 2 (a). The simulation is close to the experiment as indicative shown with the vertical lines, showing reduced reflectivity where SPPs are excited. An additional feature is appearing in the calculation at  $\approx 3.1$  eV that originates from the splitting of the plasmonic excitation in different directions as we move away from the normal incidence. Experimentally, we hardly see these dips in the reflectivity curves due to their lower relative intensity in combination with the smaller resolving power of our reflectivity setup.

From Fig. 2 (a,c) we see that the reflectance minima exhibit a red shift in energies as we change the thickness from 20 to 100 nm. For example, the three minima of reflectivity for the sample of 60 nm are located at  $\approx 2.81$ ,  $\approx 3.2$  (calculation) and  $\approx 4.0$  eV. On the contrary the three minima of reflectivity for the sample of 100 nm are at  $\approx 2.69$ ,  $\approx 3.1$  and  $\approx 3.75$  eV. All of them red shifted compared to the thinner 60 nm sample. By holding constant the size of the holes at 260 nm the critical parameter here becomes the ratio  $h/a$ , of the thickness  $h$  with respect to the period of the pattern  $a$ [18]. Increasing the thickness from 60 nm to 100 nm and the corresponding ratio from  $h/a = 0,13$  to  $h/a = 0,21$ , we observe a redshift of the reflectivity minima. Similar redshift of transmission maxima with the thickness in the presence of plasmonic excitations has been observed in antidot structures composed of Ag, and Au [18]. The presence of highly absorbing magnetic metal does not alter this behaviour revealing that the driving force of the reflection minima are the excitation of surface plasmons polaritons.

The experimental Kerr rotation spectra of the three patterned and the three reference Co samples, with different thicknesses, are presented in Fig. 2 (d). The magneto-optic response depends on the minima of reflectivity. The thinnest sample of 20 nm presenting a very small signature of SPPs signature in its reflectivity curve, does not exhibit a significant difference in the Kerr spectrum with respect to its continuous counterpart. However, the other two patterned samples show strong changes as compared to the continuous films, with extraordinary enhancement of the Kerr rotation. At the energies where SPP modes are involved, the Kerr rotation  $\theta_K$  is enhanced.  $\theta_K$  is maximized at  $\approx 2.69$ , and at  $\approx 2.81$  eV for the 100 and 60 nm respectively. A second important feature appears at energies  $\approx 3.1 - 3.2$  eV where another enhancement maximum is noticeable for both thick samples. A further surprising characteristic is the behaviour above 3.5 eV. For the 60 nm sample, the enhancement around 4 eV is strong, 3 times higher than

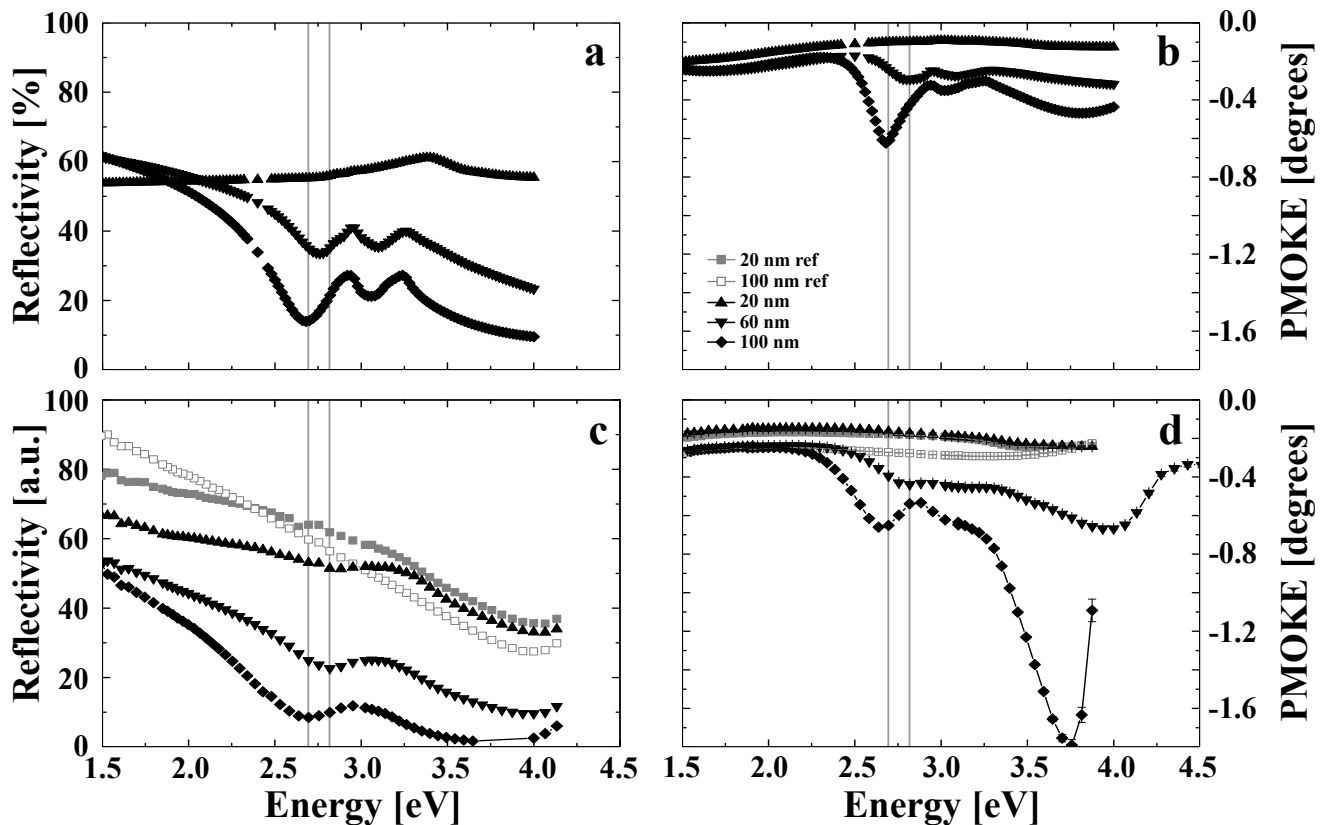


FIG. 2. Calculated reflectivity (a), experimental reflectivity (c), calculated PMOKE spectra(b), and experimental PMOKE spectra (d) for three different thicknesses of 20 nm, 60 nm and 100 nm. Black symbols refer to the patterned samples, while white symbols show the behaviour of the continuous films of the same composition. Extraordinary troughs are observed in the reflectivity. The patterned samples show clear changes in the Kerr spectra at different thicknesses. Strong enhancement of the Kerr rotation is obtained from the 60 nm and 100 nm samples at energies where SPPs are excited.

its continuous counterpart. The broad trough in reflectivity for the 100 nm sample around  $\approx 3.75$  eV gives rise to a surprising sixfold enhancement of the Kerr rotation, as compared to the continuous film at the same energy. The size of the enhancement is one of the biggest ever reported (Ref [2] and references therein). The extraordinary enhancement is correlated to the third broader and deep trough in reflectivity that appears in the energy region  $\approx 3.8 - 4.0$  eV for the two thicker samples. Reduced reflectivity at the beginning of the ultraviolet region is also a typical property of the continuous films. The impressive enhancement of the Kerr rotation depends on the plasmonic excitations and moreover it can be controlled by the thickness. Figure 2 nicely shows that the feature of enhancement does not only depend on the in-plane structuring of the sample but also on the out-of-plane geometrical parameters, such as the thickness.

The excited SPPs are correlated to the thickness through their field penetration depth. As it has been shown, the penetration depth of SPPs,  $\delta_{skin}$ , in metals is usually of the order of 10 nm in the visible and infrared [19]. Furthermore, in our case the absorbing ferromagnetic materials introduces significant losses (large intrinsic absorption). The role of overlapping SPPs field

in the magnetic layer has been previously observed in symmetric structures of Au/Co/Au [16, 20] and in Pt-capped Ag/Co/Ag structures [21]. These have revealed an optimum enhancement of the MO activity for specific Co thickness being around 7-10 nm where the excitation of the SPP in the Au layer maximises the electromagnetic field distribution in the MO Co layer for that thickness. As such, one would expect that our samples, having larger thicknesses, should have higher optical absorption and dominant damping, preventing an optimal SPP excitation and therefore a reduction in the observed MO signal. Instead, the experiment shows a maximum enhancement for the 100 nm sample. Here, we must mention that the aforementioned SP penetration depth refers to continuous trilayers and they are not to be directly compared with our antidot structures. The antidot structure and the presence of holes render the thickness parameter a very important factor for the behaviour of SPPs. As we have shown in Ref. [15] the excitations of surface plasmon polaritons in thick magnetic films leads to remarkable electric field intensity patterns that are responsible for the magneto-optic enhancement.

Although the calculation in Fig. 2 (b) captures well the size and the shape of magneto-optic enhancement in

the whole spectral region it can not reproduce the very big enhancement above  $\approx 3.75$  seen in the experiment. The reason for this is the almost zero reflectivity that is experimentally measured while in the theory the samples still have a significant percentage of reflectivity. Accordingly, the experimentally measured  $\theta_K$  depends not only on the polarization conversion due the SPPs excitations but also on the reflectivity [15]. When the reflectivity goes to zero the Kerr rotation is diverging, since the optical reflection coefficient is in the denominator [15]. The very low measured reflectivity that strongly depends on the thickness of the antidot samples significantly contributes to the very large enhancement of Kerr rotation.

In conclusion we have shown a new way to manipulate the magneto-optic response of magnetoplasmonic structures, taking advantage of the thickness of the magnetic layer. We have used patterned Co hexagonal antidot lattices with different thicknesses to generate a large enhancement of P-MOKE signal close to SPP resonances.

We have revealed that not only the in-plane struc-

ture is defining the excitation conditions for SPPs, but also the out of plane direction represented by the thickness of the magnetic layer plays a crucial role. This is further confirmed by the related PMOKE enhancement. We have shown that the thickness modifies the magneto-optic Kerr enhancement by SPPs excitation and can yield very low reflectivity values. Consequently, new routes for tailoring the functionality of patterned structures emerge, where the influence of the thickness on the magneto-optic activity has to be taken into account.

The authors would like to thank Piotr Patoka for the preparation of the polystyrene bead template. The authors acknowledge the support of the Swedish Research Council (VR), the Knut and Alice Wallenberg Foundation (KAW) and the Swedish Foundation for International Cooperation in Research and Higher Education (STINT). E. Th. P acknowledges the Carl Zeiss Foundation. A.G.-M. acknowledges funding from the Spanish Ministry of Economy and Competitiveness through grant MAT2014-58860-P, and from the Comunidad de Madrid through Contract No. S2013/MIT-2740.

- 
- [1] V. V. Temnov, G. Armelles, U. Woggon, D. Guzatov, A. Cebollada, A. García-Martín, J.-M. García-Martín, T. Thomay, A. Leitenstorfer, and R. Bratschitsch, *Nature Photonics* **4**, 107 (2010).
- [2] G. Armelles, A. Cebollada, A. García-Martín, and M. U. Gonzalez, *Advanced Optical Materials* **1**, 10 (2013).
- [3] V. I. Belotelov, I. A. Akimov, M. Pohl, V. A. Kotov, S. Kasture, A. S. Vengurlekar, G. A. Venu, D. R. Yakovlev, A. K. Zvezdin, and M. Bayer, *Nature Nanotech.* **4**, 1 (2011).
- [4] D. Martín-Becerra, J. B. Gonzalez-Díaz, V. V. Temnov, A. Cebollada, G. Armelles, T. Thomay, A. Leitenstorfer, R. Bratschitsch, A. García-Martín, and M. U. Gonzalez, *Applied Physics Letters* **97**, 183114 (2010).
- [5] E. T. Papaioannou, T. Meyer, and B. Hillebrands, *Journal of Surfaces and Interfaces of Materials* **2**, 40 (2014).
- [6] L. Chen, J. Gao, W. Xia, S. Zhang, S. Tang, W. Zhang, D. Li, X. Wu, and Y. Du, *Phys. Rev. B* **93**, 214411 (2016).
- [7] E. Melander, E. Östman, J. Keller, J. Schmidt, E. T. Papaioannou, V. Kapaklis, U. B. Arnalds, B. Caballero, A. García-Martín, J. C. Cuevas, and B. Hjörvarsson, *Applied Physics Letters* **101**, 063107 (2012).
- [8] E. T. Papaioannou, V. Kapaklis, P. Patoka, M. Giersig, P. Fumagalli, A. García-Martín, E. Ferreira-Vila, and G. Ctistis, *Phys. Rev. B* **81**, 054424 (2010).
- [9] E. T. Papaioannou, V. Kapaklis, E. Melander, B. Hjörvarsson, S. D. Pappas, P. Patoka, M. Giersig, P. Fumagalli, A. García-Martín, and G. Ctistis, *Opt. Express* **19**, 23867 (2011).
- [10] G. Ctistis, E. Papaioannou, P. Patoka, J. Gutek, P. Fumagalli, and M. Giersig, *Nano Lett.* **9**, 1 (2009).
- [11] A. V. Chetvertukhin, A. A. Grunin, T. V. Dolgova, M. Inoue, and A. A. Fedyanin, *J. Appl. Phys.* **113**, 17A942 (2013).
- [12] D. M. Newman, M. L. Wears, R. J. Matelon, and I. R. Hooper, *Journal of Physics: Condensed Matter* **20**, 345230 (2008).
- [13] N. Maccaferri, X. Inchausti, A. Garca-Martn, J. C. Cuevas, D. Tripathy, A. O. Adeyeye, and P. Vavassori, *ACS Photonics* **2**, 1769 (2015), <http://dx.doi.org/10.1021/acsphotonics.5b00490>.
- [14] N. Maccaferri, L. Bergamini, M. Pancaldi, M. K. Schmidt, M. Kataja, S. v. Dijken, N. Zabalá, J. Aizpurua, and P. Vavassori, *Nano Letters* **16**, 2533 (2016), pMID: 26967047, <http://dx.doi.org/10.1021/acs.nanolett.6b00084>.
- [15] M. Rollinger, P. Thielen, E. Melander, E. Östman, V. Kapaklis, B. Obry, M. Cinchetti, A. García-Martín, M. Aeschlimann, and E. T. Papaioannou, *Nano Letters* **16**, 2432 (2016), pMID: 27018661, <http://dx.doi.org/10.1021/acs.nanolett.5b05279>.
- [16] G. Armelles, A. Cebollada, A. García-Martín, J. M. García-Martín, M. U. González, J. B. González-Díaz, E. Ferreira-Vila, and J. F. Torrado, *J. Opt. A: Pure Appl. Opt.* **11**, 114023 (2009).
- [17] B. Caballero, A. García-Martín, and J. Cuevas, *Phys. Rev. B* **85**, 245103 (2012).
- [18] L. Martín-Moreno, F. J. García-Vidal, H. J. Lezec, K. M. Pellerin, T. Thio, J. B. Pendry, and T. W. Ebbesen, *Phys. Rev. Lett.* **86**, 1114 (2001).
- [19] V. V. Temnov, *Nat Photon* **6**, 872 (2012).
- [20] J. B. González-Díaz, A. García-Martín, G. Armelles, J. M. García-Martín, C. Clavero, A. Cebollada, R. A. Lukaszew, J. R. Skuza, D. P. Kumah, and R. Clarke, *Phys. Rev. B* **76**, 153402 (2007).
- [21] E. Ferreira-Vila, J. B. González-Díaz, R. Fermento, M. U. González, A. García-Martín, J. M. García-Martín, A. Cebollada, G. Armelles, D. Meneses-Rodríguez, and E. M. n. Sandoval, *Phys. Rev. B* **80**, 125132 (2009).